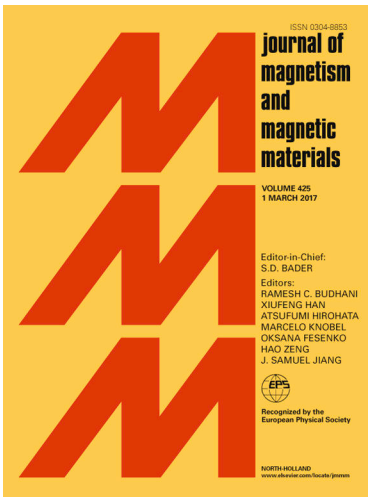

Magnetocaloric effect in nanocrystalline manganite bilayer thin films

S. Passanante, L.P. Granja, C. Albornoz, D. Vega, D. Goijman, M.C. Fuertes, C. Ferreyra, L. Ghivelder, F. Parisi, M. Quintero

PII: S0304-8853(22)00466-8
DOI: https://doi.org/10.1016/j.jmmm.2022.169545
Reference: MAGMA 169545

To appear in: *Journal of Magnetism and Magnetic Materials*

Received Date: 6 January 2022
Revised Date: 17 May 2022
Accepted Date: 26 May 2022

Please cite this article as: S. Passanante, L.P. Granja, C. Albornoz, D. Vega, D. Goijman, M.C. Fuertes, C. Ferreyra, L. Ghivelder, F. Parisi, M. Quintero, Magnetocaloric effect in nanocrystalline manganite bilayer thin films, *Journal of Magnetism and Magnetic Materials* (2022), doi: https://doi.org/10.1016/j.jmmm.2022.169545

Magnetocaloric effect in nanocrystalline manganite bilayer thin films

S. Passanante[1,2,3], L. P. Granja[1,2], C. Albornoz[1], D. Vega[1,3], D. Goijman[2,4], M. C. Fuertes[2,5], C. Ferreyra[1,2], L. Ghivelder[6], F. Parisi[1,7], M. Quintero[1,2,3,*]

[1] Departamento de Física de la Materia Condensada, Gerencia de Investigación y Aplicaciones, Centro Atómico Constituyentes, Comisión Nacional de Energía Atómica, Av. Gral. Paz 1499 (B1650KNA), San Martín, Buenos Aires, Argentina.

[2] Instituto de Nanociencia y Nanotecnología, CONICET-CNEA, Av. Gral. Paz 1499 (B1650KNA), San Martín, Buenos Aires, Argentina.

[3]Instituto Sabato/ Escuela de Ciencia y Tecnología, UNSAM

[4]Comisión Nacional de Energía Atómica (CNEA); Consejo Nacional de Investigaciones Científicas y Técnicas (CONICET), Centro Atómico Bariloche, Universidad Nacional de Cuyo (UNCUYO); Av. Bustillo 9500, R8402AGP San Carlos de Bariloche, Argentina

[5] Gerencia Química, Centro Atómico Constituyentes, Comisión Nacional de Energía Atómica, Av. Gral. Paz 1499(B1650KNA), San Martín, Buenos Aires, Argentina.

[6]Instituto de Fisica, Universidade Federal do Rio de Janeiro, 21941-972 Rio de Janeiro, RJ, Brazil

[7] Instituto de Ciencias Físicas, Escuela de Ciencia y Tecnología, UNSAM, Alem 3901, San Martín (1650), Buenos Aires, Argentina

* Corresponding Author at: Departamento de Física de la Materia Condensada, CAC, CNEA, Av. Gral Paz 1499, San Martín 1650, Argentina
E-mail address: mquinter@cnea.gov.ar

Highlights:

- We studied the magnetocaloric effect in polycrystalline bilayers thin films of $La_{1-x}Sr_xMnO_3$, deposited by pulse laser deposition on silicon substrates.
- The temperature range where the magnetocaloric effect develops is enhanced.
- MCE is independent of the stacking sequence and the substrate of the films.
- It is possible to combine the magnetocaloric effect qualities of nanocomposites and thin films.

Due to their large surface-volume ratio, thin films are good candidates for magnetocaloric effect applications in refrigeration devices. With this aim, we studied the magnetic and magnetocaloric properties of the bilayers manganite thin films, $La_{0.88}Sr_{0.12}MnO_3$ / $La_{0.75}Sr_{0.25}MnO_3$ and $La_{0.75}Sr_{0.25}MnO_3$ / $La_{0.88}Sr_{0.12}MnO_3$, and their control single layer films, $La_{0.75}Sr_{0.25}MnO_3$ and $La_{0.88}Sr_{0.12}MnO_3$. These films were grown by pulsed laser deposition on silicon substrates, resulting in polycrystalline films with average grain size of ~35nm. We found that, for the bilayers, the temperature range of the magnetocaloric effect can be broadened without reducing the refrigerant capacity. Therefore, it is possible to combine the magnetocaloric effect qualities of nanocomposites and thin films in order to improve the performance and expand their potential use in refrigeration devices

Keywords

Magnetocaloric Effect / Thin films/ Polycrystalline / Manganites/ Bilayers

The magnetocaloric effect (MCE) is known as the adiabatic temperature (T) change in a material when a magnetic field is applied [1], and can be indirectly evaluated from the magnetic entropy change $\Delta S_M(T)$. Both magnitudes are related through the expression as $\Delta T_{ad} = -\frac{T}{C}\Delta S_M$ [1], where C is the specific heat of the material. The main motivation to study the MCE is the possibility to design and build new refrigeration devices based on this phenomenon. In 1997 Pecharsky and Gschneidner found giant MCE in $Gd_5(Si_xGe_{1-x})_4$ alloys at room temperature [2] [3]. This discovery sparked a great interest in the scientific community looking for optimal materials for solid state refrigeration. In that sense, new compounds were proposed, like Mn based samples [4], Heusler alloys [5],

LaFe (Si, Al) systems [6], and mixed valence manganese oxides, called manganites [7] [8].

Manganites are perovskites of general formula $R_{1-x}A_xMnO_3$, where R is a rare earth element and A is an alkaline metal. Using different combinations of these elements it is possible to obtain compounds with very different properties. Additionally, the strong coupling between magnetic, electronic, and structural properties, promotes large entropy changes with moderate magnetic fields [7]. Therefore, manganites are good candidates for MCE based devices, and their behavior has been thoroughly studied in bulk systems [9] [10] [11] [12]. Particularly for the $La_{1-x}Sr_xMnO_3$ family (LSMO), the ferromagnetic Curie temperature, T_C, can be tuned within a broad temperature range, including room temperature, by choosing an appropriate proper Sr content [13]. Since the maximum magnetic entropy change is reached at T_c [7] [14], the LSMO system appears to be a good candidate for devices operating in the vicinity of room temperature.

Although part of the MCE community is focused on developing a macroscopic refrigerator apparatus, in order to introduce an ecological alternative to the current gas-based refrigeration systems [14] [15], other efforts are directed to micro and nanodevices, to meet specific refrigeration requirements [16]. When the scale is reduced, the influence of the morphology and the device geometry on the MCE-based properties becomes fundamental to improve the heat exchange for MCE applications [17] [18] [19] [20]. Within this context, an important parameter for MCE devices design is the temperature range where the effect is appreciable. A strategy to increase the temperature range of the MCE is the use of composite materials [21] [22]. Composite-based devices have shown

the capability to enhance the MCE temperature width due to their inherent microstructure, in which T_C is spatially defined by the local composition. Thus, grain size is a relevant parameter to define the MCE properties in composites [22].

However, a disadvantage of powder composites is that heat exchange mainly develops between grains of different compositions, which results in a lack of efficiency for the MCE. Thus, other strategies to widen the temperature range of MCE is by using multilayer thin films for the design of micro and nanodevices for magnetic refrigeration [16]. It was demonstrated that thin films can improve the temperature span, and their geometry optimizes the heat exchange between the active material and the surroundings, decreasing the duration of the cooling cycles [17] [23]. In the case of multilayers, it is expected that each layer contributes independently to the MCE. Thus, by stacking layers of different composition it would be possible to yield a device with an expanded temperature range and sizable MCE. In the case of epitaxial thin film multilayers, the stacking sequence and stress induced by the substrate affect both the magnitude and temperature range of the MCE [24] [25].

In this work we explored the MCE in $La_{0.88}Sr_{0.12}MnO_3$ (LSMO12) and $La_{0.75}Sr_{0.25}MnO_3$ (LSMO25) single and bilayers thin films, deposited by pulsed laser ablation on silicon substrates. A schematic diagram of the studied samples is shown in Fig. 1. We analyzed the influence of the morphological parameters of the studied compounds on the magnetic properties, magnetic entropy change, and temperature width, relevant for the MCE. We demonstrate that the nanocrystalline structure induced by this technology friendly substrate combines the advantages of thin films and nanocomposites.

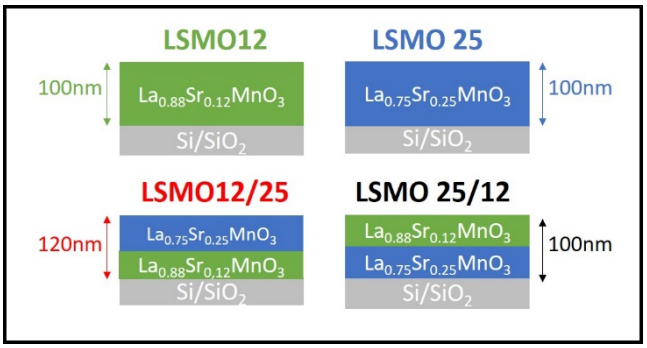

Figure 1 **(color should be used in print)**: Sketched illustrating the composition, denomination and thickness of the samples studied. In the case of the bilayers, the thickness corresponds to the whole film including, both compounds.

Experimental

Thin films of $La_{1-x}Sr_xMnO_3$, with x = 0.12 and x = 0.25, were deposited by pulsed laser deposition using the 266 nm harmonic of a Nd:YAG laser with a pulse frequency of 10 Hz and a fluence of 1 J/cm^2. The deposition conditions were 850°C and 0.1 mbar of O_2 pressure. After the deposition, the film was cooled to room temperature at 100 mbar of O_2, in order to reduce the amount of oxygen vacancies and improve its magnetic properties [26]. The LSMO films were deposited on 1µm thermal oxide Si substrates, resulting in Volmer-Weber type polycrystalline growth [27].

Grazing incidence X-ray diffraction (XRD) and X-ray reflectometry (XRR) measurements were performed using a Panalytical Empyrean diffractometer, in

order to determine the crystalline structure and the thickness of the films. Morphology was characterized by scanning electron microscopy (SEM). Magnetization as a function of the temperature and magnetic field (+/- 3000 Oe), applied parallel to the substrate, was measured in a commercial vibrating sample magnetometer Versalab (50 K – 400 K) and a PPMS (10 K – 400 K), both manufactured by Quantum Design.

Results and discussion

From XRD results (Fig. 2a) we studied the structural properties of the samples. It was observed a pseudo cubic polycrystalline structure with a lattice parameter $a \approx 3.88$ Å for all the samples. XRR for the bilayer films displayed the interference pattern associated to the total thickness of the sample. It is not being possible to distinguish one layer from the other due to their similar electronic densities (Fig. 2b). This fact was confirmed by cross section SEM images (Fig. 2c) where only the interface with the substrate is visible, but no interface between LSMO12 and LSMO25 can be distinguished. The SEM image in Fig. 2d confirms the polycrystalline growth, showing the presence of grains. From these images we

calculated an average grain size of 35 nm on the surface of the thin films (inset of Fig. 2d).

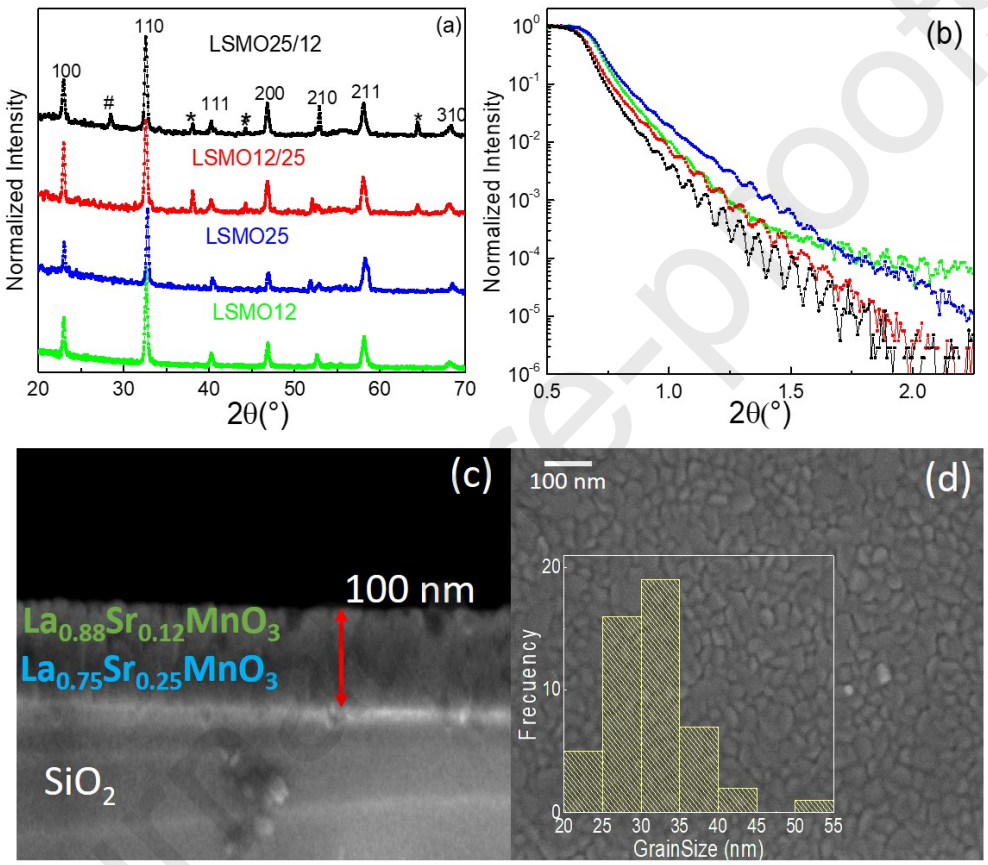

Figure 2**(color should be used in print)**: (a) XRD patterns for single layer thin films (LSMO12 and LSMO25) and for bilayers thin films (LSMO12/25 and LSMO25/12). Additional Bragg peaks in LSMO12/25 and LSMO25/12 correspond to silicon (#) [28] and metallic Ag (*) [29], corresponding to the silicon substrate and the silver paint used to stick the substrate to the heater during the PLD deposition of the film, respectively. (b) XRR measurements for both bilayer thin films and single layer thin films. (c) SEM image for LSMO2512

cross section showing no evidence of the interface. (d) SEM image for LSMO1225. Inset: grain size distribution.

Field cooled magnetization measurements with H = 1000 Oe are shown in Fig. 3. For the bilayer films, two bumps are observed, which agree with the paramagnetic (PM) to ferromagnetic (FM) transition temperatures T_C of the corresponding single layer films (175 K for LSMO12 and 295 K for LSMO25). The Inset of Fig. 3 displays the derivative , $\partial M/\partial T$, in order to compare the PM-FM transitions of the films with the presence of both transitions in the bilayers.

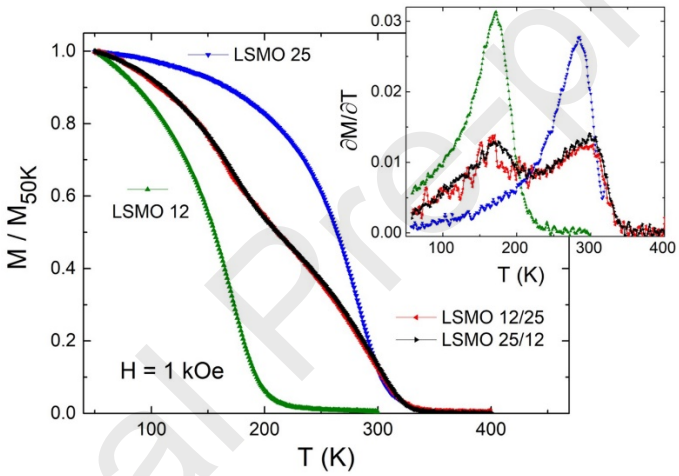

Figure 3 **(color should be used in print)**: Magnetization normalized at 50K (M/M_{50K}) versus temperature (T) of the single layer (LSMO12, LSMO25) and the bilayer (LSMO1225, LSMO2512) films. Inset: Derivative, $\partial M/\partial T$, as a function of T.

Measurements of M(H) present a typical FM hysteresis behavior for all samples, as shown in Fig. 4 at 50 K. As can be observed in Figs. 3 and 4, the magnetic behavior of the bilayer samples is independent of the stacking order of the layers. The inset of Fig. 4 displays the temperature dependence of the coercive field H_c.

It decreases to $H_c = 0$ near T_C, as expected. This results in a smaller magnetic hysteresis at low temperatures than the reported for other magnetic materials [30] [31]. No trace of two separate coercive fields appears at low temperatures for the bilayers, suggesting a FM coupling between layers, resulting in a single and still abrupt H_c, whose values lies between the ones for the single layers.

It can be observed in Fig. 4 that a magnetic field of 1000 Oe is enough to saturate the magnetization of all films. This reduces the energy needed to perform a refrigeration cycle, an advantage over bulk manganites [32]. The saturation magnetization, M_{SAT}, is smaller than the expected values, 3.88 μ_B/Mn and 3.75 μ_B/Mn for x= 0.12 an x =0.25 respectively. This difference is attributed to magnetic disorder at the surface of the grains, resulting in a magnetic dead layer of $\sim$ 2 nm for each grain [33]. The grain surface favors the presence of oxygen vacancies, generating antiferromagnetic Mn^{+2}-Mn^{+2} bonds, which compete with the Mn^{+3}-O-Mn^{+4} double exchange interaction. Furthermore, the FM grain core is surrounded by a magnetically frustrated surface state [34] [35] [36]. Additional evidence of magnetic frustration at the dead layer is the considerable difference between the field-cooled-warming and zero-field-cooled magnetization measurements (Fig.5). Note that these measurements were performed with H=500 Oe which is higher than H_c(T) (see Inset of Fig. 4) in order to avoid coercive field effects [37].

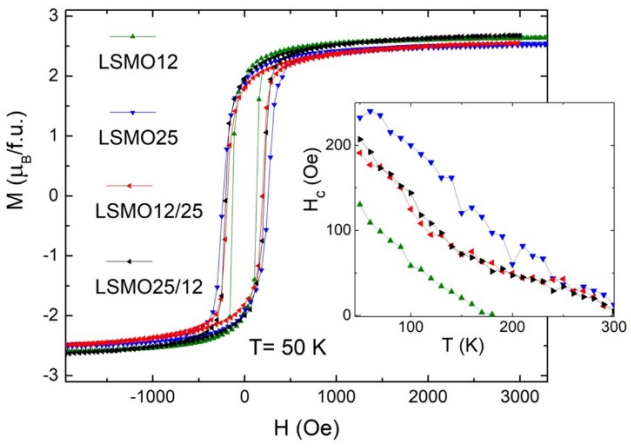

Figure 4 **(color should be used in print)**: Magnetization M versus applied magnetic field H measured at T = 50 K for the LSMO films. Inset: temperature dependence of the coercive field H_c extracted from the M(H) curves measured at different temperatures.

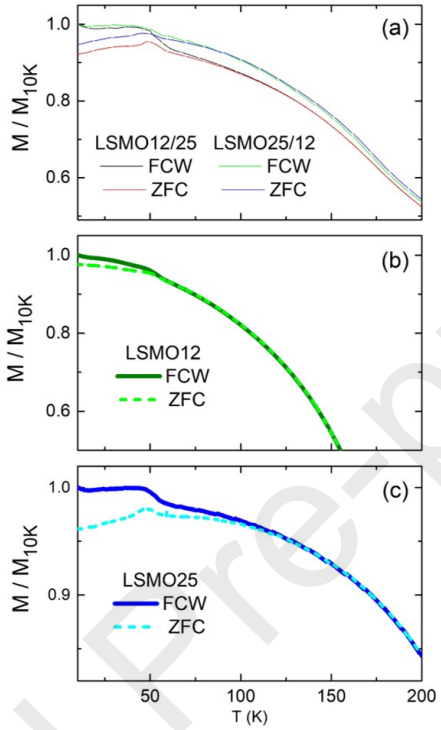

Figure 5 **(color should be used in print)**: Comparison between the field cooled warming (FCW) and the zero-field cooled (ZFC) M(T) results measured at H=500 Oe for (a) the bilayers, (b) LSMO12 and (c) LSMO25. Note: The presence of the peak around 50 K is due to oxygen contamination inside the MPMS chamber [38].

In order to study the MCE, M(H) curves were measured at different temperatures, and the isothermal magnetic entropy change ΔS_M was calculated with the expression $\Delta S_M = \frac{1}{\Delta T}\int_0^H [M(H',T+\Delta T) - M(H',T)]dH'$. Figure 6 displays $-\Delta S_M(T)$ obtained with H=3000 Oe. It can be observed that for LSMO12 and LSMO25, the maximum of $-\Delta S_M(T)$ coincides with T_C. In the case of the bilayers, two well distinguished peaks appear, associated to each layer transition temperature. This feature was previously reported for epitaxial bilayer

manganite thin films [25], where the MCE is strongly influenced by the strain mismatch with the substrate. In contrast, in our study, $\Delta S_M(T)$ is independent of the stacking sequence of the films for polycrystalline bilayers, expanding the possibilities for the combination of chemical compounds in the multilayers. Since only about half of the film thickness is contributing to the MCE at each T_C, the apparent reduction in the magnitude of -$\Delta S_M(T)$ for the bilayers is mainly an artifact related to the mass normalization of the sample. A similar behavior can be observed for the magnetization derivative (inset of Fig. 3). The adiabatic temperature change for each layer should be comparable to the corresponding single layer film. In order to confirm this fact, inset of Fig. 6 displays the addition of the curves of -$\Delta S_M(T)$ obtained for LSMO12 and LSMO25 (Note that 0.5 correction factor was needed due to the thickness difference between the single layer and bilayer samples). Comparing with the one obtained for LSMO2512, the behavior of both curves are very similar. However, within the temperature range between the transitions of both single layers, -$\Delta S_M(T)$ is larger for LSMO2512 as compared with LSMO12+25. This effect would suggest the presence of magnetic inhomogeneities originated on a gradient of compositions at the interface between LSMO12 and LSMO25 [39] [40]. The temperature range where the effect develops is usually determined by the full width at half maximum (δT_{FWHM}) of -$\Delta S_M(T)$. In the case of the bilayers, they present two well distinguishable peaks. In order to calculate their δT_{FWHM}, it was considered the lower T bound of δT_{FWHM} of the peak at 170K and the higher T bound of δT_{FWHM} of the peak at 300K, following the criteria previously reported in [25].

Table 1 displays T_C and δT_{FWHM} extracted from the results of Fig. 6. An important increment of δT_{FWHM} for the films compared with bulk samples is observed, associated with the broadening of the PM-FM transition in the thin films. Smaller grain size and oxygen vacancies present in the films are responsible for this effect [41]. Within this context, temperature averaged entropy change (TEC) is usually evaluated to compare the MCE properties of the materials [42]. It can be estimated from $\Delta S_M(T)$ curves as $TEC(\Delta T_{lift}) = \frac{1}{\Delta T_{lift}} max \left\{ \int_{T_{mid}-\frac{\Delta T_{lift}}{2}}^{T_{mid}+\frac{\Delta T_{lift}}{2}} |\Delta S_M| dT \right\}$, where T_{mid} is selected to maximize TEC and ΔT_{lift} was

chosen to be 10 K (TEC(10)). Table 1 shows the values of TEC (10) calculated for all the thin films and bulk samples for 3000 Oe. These results are in good agreement with others perovskite systems [43] [44] [45] [46] [47]. Moreover, the temperature range where the MCE becomes important for the bilayers is almost twice the single layer ones, including both $\Delta S_M(T)$ peaks at each T_C. They are separated by an intermediate interval of T where $\Delta S_M(T)$ does not depend on temperature. This fact could be exploited in the design of a refrigeration device with a constant performance within the temperature interval between the transitions.

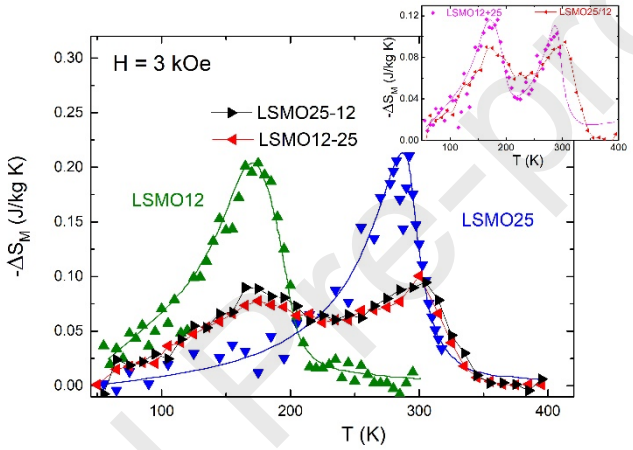

Figure 6 **(color should be used in print)**: Isothermal change of the magnetic entropy (-ΔS) vs T, obtained at H= 3000 Oe. Lines are guides for the eye. Inset: Comparison between -$\Delta S_M(T)$ for LSMO25+12 and LSMO1225.

Sample Name	Tc [K]	-ΔS_{Max} [J/kg K]	δT_{FWHM} [K]	RC [J/kg]	TEC (10) [J/kg K]
LSMO12	170	0.20	73	12	0.67
LSMO25	295	0.21	60	11	0.67
LSMO12/25	170 / 300	0.09 / 0.09	200 (*)	14 (*)	0.27/0.33

LSMO25/12	170 / 300	0.09 / 0.09	200 (*)	15 (*)	0.3/0.3
Bulk x = 0.12 [17]	290	0.47	27	10	1.17
Bulk x = 0.25	345	0.55	21	8	1.3

Table 1: Comparison between Tc, δT_{FWHM}, -ΔS_{max}, TEC (10) and RC for the thin films and their corresponding bulks. (*) Note: for the bilayers, it was considered the lower T bound of δT_{FWHM} of the peak at 170K and the higher T bound of δT_{FWHM} of the peak at 300K.

The refrigerant capacity (RC) is a usual way to quantify how good a system is for refrigeration, defined as $RC = -\int_{T_1}^{T_2} \Delta S_M dT$ [48]. This quantity expresses how much heat is transferred from the hot reservoir (T_2) to the cold one (T_1) in an ideal refrigeration cycle. These temperatures, T_1 and T_2, are chosen to correspond with the δT_{FWHM}. Table 1 shows the RC for all films, which are in good agreement with values previously reported [17]. Furthermore, it can also be estimated from the addition of -$\Delta S_M(T)$ for LSMO12 and LSMO25, as displayed in the Inset of Fig. 6., which yield RC = 12.5 J/Kg. It can be observed for the bilayers that RC is slightly larger than the value obtained for the single layer films and LSMO25+12. This result suggests that the RC increment for the bilayers is mainly due to the magnetic inhomogeneities between the PM-FM transition temperatures of LSMO25 and LSMO12 films.

An alternative strategy widely explored to expand δT_{FWHM} is the composites of polycrystalline powders [49] [50] which allows the mix of different chemical compositions to establish a working temperature range of interest. Particularly, an improvement of the MCE characteristics, relative to the bulk composite of the

same compounds, was previously reported for nanocrystalline manganite composites with grain size comparable to the one of the films displayed here [22]. In that case a unique broad $-\Delta S_M(T)$ peak of the same order of magnitude of our bilayers was observed (see Table 1), in contrast with the two well distinguished peaks observed in our bilayer thin films. Moreover, thin films are more efficient than composite morphology for heat exchange.

Conclusions

This work reports the magnetocaloric properties of nanocrystalline bilayers manganite thin films, deposited by PLD on silicon substrates. These multilayer thin films present low saturation field and small magnetic hysteresis, which are important conditions for MCE applications. In contrast to manganites nanocomposites powders, the spread of the temperature range of $\Delta S_M(T)$ shows two well distinguished peaks corresponding to the transition temperatures of each layer. It was previously attributed to a characteristic of epitaxial multilayer thin films and composites, with grain size greater than hundreds of nm. However, in contrast with epitaxial thin films, no interfacial strain effect is present, and the

MCE is independent of the stacking sequence and the substrate of the films, for nanocrystalline multilayers thin films [25].

Thus, we have demonstrated that it is possible to combine the advantages of thin films and nanocomposites. On one hand, it is possible to increase the temperature range where the magnetocaloric effect develops. On the other hand, thin films morphology can be exploited to optimize the heat exchange.

Moreover, fabrication conditions for polycrystalline thin films allow access to larger substrates and the incorporation of any intermediate layer between the MCE compounds, as a dissipation material or as the one to be refrigerated. Therefore, this work opens the path to more versatile designs for micro and nanoscale applications.

Acknowledgements

The authors gratefully acknowledge financial support received from ANPCyT (PICT 2014-2116 and 2018-2397). LG acknowledges financial support from the Brazilian agencies FAPERJ and CNPq. We thank CMA belonging to the Sistema Nacional de Microscopía (MINCYT).

References

[1] A. M. Tishin, The magnetocaloric effect and its applications, Bristol Philadelphia: Institute of Physics Pub, 2003.

[2] V. K. Pecharsky and J. K. A. Gschneidner, «Giant Magnetocaloric Effect inGd5(Si2Ge2),» *Physical Review Letters,* vol. 78, p. 4494–4497, 6 1997.

[3] V. K. Pecharsky and K. A. Gschneidner, «Effect of alloying on the giant magnetocaloric effect of Gd5(Si2Ge2),» *Journal of Magnetism and Magnetic Materials,* vol. 167, p. L179–L184, 3 1997.

[4] H. Wada and Y. Tanabe, «Giant magnetocaloric effect of MnAs1-xSbx,» *Applied Physics Letters,* vol. 79, p. 3302–3304, 11 2001.

[5] A. Planes, L. Mañosa, X. Moya, T. Krenke, M. Acet and E. F. Wassermann, «Magnetocaloric effect in Heusler shape-memory alloys,» *Journal of Magnetism and Magnetic Materials,* vol. 310, p. 2767–2769, 3 2007.

[6] B. G. Shen, J. R. Sun, F. X. Hu, H. W. Zhang and Z. H. Cheng, «Recent Progress in Exploring Magnetocaloric Materials,» *Advanced Materials,* vol. 21, p. 4545–4564, 12 2009.

[7] M.-H. Phan and S.-C. Yu, «Review of the magnetocaloric effect in manganite materials,» *Journal of Magnetism and Magnetic Materials,* vol. 308, p. 325–340, 1 2007.

[8] A. Rebello, V. B. Naik and R. Mahendiran, «Large reversible magnetocaloric effect in La0.7-xPrxCa0.3MnO3,» vol. 110, p. 013906, July 2011.

[9] Y. Sun, X. Xu and Y. Zhang, «Large magnetic entropy change in the colossal magnetoresistance material La2/3Ca1/3MnO3,» *Journal of Magnetism and Magnetic Materials,* vol. 219, p. 183–185, 9 2000.

[10] A. Szewczyk, M. Gutowska, B. Dabrowski, T. Plackowski, N. P. Danilova and Y. P. Gaidukov, «Specific heat anomalies in La1-xSrxMnO3 (0.12≤x≤0.2),» *Physical Review B,* vol. 71, 6 2005.

[11] M. Quintero, J. Sacanell, L. Ghivelder, A. M. Gomes, A. G. Leyva and F. Parisi, «Magnetocaloric effect in manganites: Metamagnetic transitions for magnetic refrigeration,» *Applied Physics Letters,* vol. 97, p. 121916, 9 2010.

[12] M. Quintero, S. Passanante, I. Irurzun, D. Goijman and G. Polla, «Grain size modification in the magnetocaloric and non-magnetocaloric transitions in La0.5Ca0.5MnO3 probed by direct and indirect methods,» *Applied Physics Letters,* vol. 105, p. 152411, 10 2014.

[13] M. B. Salamon y M. Jaime, «The physics of manganites: Structure and transport,» *Reviews of Modern Physics,* vol. 73, p. 583–628, 8 2001.

[14] A. Kitanovski, J. TuSek, U. Tomc, U. Plaznik and M. Ozbolt, Magnetocaloric Energy Conversion, Springer-Verlag GmbH, 2014.

[15] T. Gottschall, K. P. Skokov, M. Fries, A. Taubel, I. Radulov, F. Scheibel, D. Benke, S. Riegg and O. Gutfleisch, «Making a Cool Choice: The Materials Library of Magnetic Refrigeration,» *Advanced Energy Materials,* vol. 9, p. 1901322, July 2019.

[16] J. H. Belo, A. L. Pires, J. P. Araújo and A. M. Pereira, «Magnetocaloric materials: From micro- to nanoscale,» *Journal of Materials Research,* vol. 34, p. 134–157, November 2018.

[17] P. Lampen, N. S. Bingham, M. H. Phan, H. Kim, M. Osofsky, A. Piqué, T. L. Phan, S. C. Yu and H. Srikanth, «Impact of reduced dimensionality on the magnetic and magnetocaloric response of La0.7Ca0.3MnO3,» *Applied Physics Letters,* vol. 102, p. 062414, 2 2013.

[18] C. W. Miller, D. D. Belyea and B. J. Kirby, «Magnetocaloric effect in nanoscale thin films and heterostructures,» *Journal of Vacuum Science & Technology A: Vacuum, Surfaces, and Films,* vol. 32, p. 040802, July 2014.

[19] S. K. Vandrangi, J.-C. Yang, Y.-M. Zhu, Y.-Y. Chin, H.-J. Lin, C.-T. Chen, Q. Zhan, Q. He, Y.-C. Chen and Y.-H. Chu, «Enhanced Magnetocaloric Effect Driven by Interfacial Magnetic Coupling in Self-Assembled Mn3O4–La0.7Sr0.3MnO3 Nanocomposites,» *ACS Applied Materials & Interfaces,* vol. 7, p. 26504–26511, November 2015.

[20] M. Pękała, «Magnetic field dependence of magnetic entropy change in nanocrystalline and polycrystalline manganites La1-xMxMnO3 (M=Ca,Sr),» *Journal of Applied Physics,* vol. 108, p. 113913, December 2010.

[21] A. G. Gamzatov, A. M. Aliev and A. R. Kaul, «Magnetocaloric effect in La1-xKxMnO3 (x = 0.11, 0.13, 0.15) composite structures in magnetic fields up to 80 kOe,» vol. 710, p. 292–296, July 2017.

[22] M. Pękała, K. Pękała, V. Drozd, K. Staszkiewicz, J.-F. Fagnard and P. Vanderbemden, «Magnetocaloric and transport study of poly- and nanocrystalline composite manganites La0.7Ca0.3MnO3/La0.8Sr0.2MnO3,» *Journal of Applied Physics,* vol. 112, p. 023906, 7 2012.

[23] A. M. Pereira, J. C. R. E. Oliveira, J. C. Soares, J. Ventura, J. B. Sousa and J. P. Araújo, «Simulations of refrigeration on integrated circuits using micro-channels,» *Journal of Non-Crystalline Solids,* vol. 354, p. 5295–5297, 12 2008.

[24] X. Moya, L. E. Hueso, F. Maccherozzi, A. I. Tovstolytkin, D. I. Podyalovskii, C. Ducati, L. C. Phillips, M. Ghidini, O. Hovorka, A. Berger, M. E. Vickers, E. Defay, S. S. Dhesi and N. D. Mathur, «Giant and reversible extrinsic magnetocaloric effects in La0.7Ca0.3MnO3 films due to strain,» *Nature Materials,* vol. 12, p. 52–58, October 2012.

[25] R. Yuan, P. Lu, H. Han, D. Xue, A. Chen, Q. Jia and T. Lookman, «Enhanced magnetocaloric performance in manganite bilayers,» *Journal of Applied Physics,* vol. 127, p. 154102, 4 2020.

[26] S. Passanante, D. Goijman, M. L. Moreau, A. G. Leyva, C. Albornoz, D. Rubi, C. Ferreyra, D. Vega, L. Granja and M. Quintero, «Magnetocaloric Effect in La0.88Sr0.12MnO3 films,» *Materials Today: Proceedings,* vol. 14, p. 104–108, 2019.

[27] T.-M. Chang and E. A. Carter, «Mean-field theory of heteroepitaxial thin metal film morphologies,» *Surface Science,* vol. 318, p. 187–203, 10 1994.

[28] S. R. Lee, K. M. Ahn and B. T. Ahn, «Silicon Epitaxial Growth on Poly-Si Film by HWCVD for Low-Temperature Poly-Si TFTs,» *Journal of The Electrochemical Society,* vol. 154, p. H778, 2007.

[29] L. Sun, Z. Zhang and H. Dang, «A novel method for preparation of silver nanoparticles,» *Materials Letters,* vol. 57, p. 3874–3879, August 2003.

[30] D. Matte, M. de Lafontaine, A. Ouellet, M. Balli and P. Fournier, «Tailoring the Magnetocaloric Effect in La2NiMnO6 Thin Films,» *Physical Review Applied,* vol. 9, 5 2018.

[31] W. Bouzidi, T. Bartoli, R. Sedek, A. Bouzidi, J. Moscovici and L. Bessais, «Low-field magnetocaloric effect of NdFe11Ti and SmFe10V2compounds,» *Journal of Materials Science: Materials in Electronics,* vol. 32, p. 10579–10586, 3 2021.

[32] M. Paraskevopoulos, F. Mayr, J. Hemberger, A. Loidl, R. Heichele, D. Maurer, V. Müller, A. A. Mukhin and A. M. Balbashov, «Magnetic properties and the phase diagram of La1-xSrxMnO3 for x≤0.2,» *Journal of Physics: Condensed Matter,* vol. 12, p. 3993–4011, 5 2000.

[33] L. J. Sinnamon, M. M. Saad, R. M. Bowman and J. M. Gregg, «Exploring grain size as a cause for dead-layer effects in thin film capacitors,» *Applied Physics Letters,* vol. 81, p. 703–705, 7 2002.

[34] S. Majumdar and S. van Dijken, «Pulsed laser deposition of La1-xSrxMnO3: thin-film properties and spintronic applications,» *Journal of Physics D: Applied Physics,* vol. 47, p. 034010, 12 2013.

[35] J. Curiale, M. Granada, H. E. Troiani, R. D. Sánchez, A. G. Leyva, P. Levy and K. Samwer, «Magnetic dead layer in ferromagnetic manganite nanoparticles,» *Applied Physics Letters,* vol. 95, p. 043106, 7 2009.

[36] N. Mottaghi, R. B. Trappen, S. Kumari, C.-Y. Huang, S. Yousefi, G. B. Cabrera, M. Aziziha, A. Haertter, M. B. Johnson, M. S. Seehra and M. B. Holcomb, «Observation and interpretation of negative remanent magnetization and inverted hysteresis loops in a thin film of La0.7Sr0.3MnO3,» *Journal of Physics: Condensed Matter,* vol. 30, p. 405804, 9 2018.

[37] N. Mottaghi, M. S. Seehra, R. Trappen, S. Kumari, C.-Y. Huang, S. Yousefi, G. B. Cabrera, A. H. Romero and M. B. Holcomb, «Insights into the magnetic dead layer in La0.7Sr0.3MnO3

thin films from temperature, magnetic field and thickness dependence of their magnetization,» *AIP Advances,* vol. 8, p. 056319, May 2018.

[38] «Quantum Design, MPMS Application Note 1014-210, https://www.qdusa.com/siteDocs/appNotes/1014-210.pdf ,1997».

[39] M. Pękała and V. Drozd, «Magnetocaloric effect in nano- and polycrystalline La0.8Sr0.2MnO3 manganites,» *Journal of Non-Crystalline Solids,* vol. 354, p. 5308–5314, December 2008.

[40] N. Mottaghi, R. B. Trappen, S. Y. Sarraf, M. S. Seehra and M. B. Holcomb, «Magnetocaloric investigations show magnetic inhomogeneity in a 7.6 nm thin film of La0.7Sr0.3MnO3/SrTiO3,» *Journal of Alloys and Compounds,* vol. 826, p. 154200, June 2020.

[41] R. Nori, S. N. Kale, U. Ganguly, N. R. C. Raju, D. S. Sutar, R. Pinto and V. R. Rao, «Morphology and Curie temperature engineering in crystalline La0.7Sr0.3MnO3 films on Si by pulsed laser deposition,» *Journal of Applied Physics,* vol. 115, p. 033518, 1 2014.

[42] L. D. Griffith, Y. Mudryk, J. Slaughter and V. K. Pecharsky, «Material-based figure of merit for caloric materials,» *Journal of Applied Physics,* vol. 123, p. 034902, January 2018.

[43] D. Mazumdar and I. Das, «Role of 3d–4f exchange interaction and local anti-site defects in the magnetic and magnetocaloric properties of double perovskite Ho2CoMnO6 compound,» *Journal of Applied Physics,* vol. 129, p. 063901, February 2021.

[44] D. Mazumdar, K. Das and I. Das, «Study of magnetocaloric effect and critical exponents in polycrystalline La0.4Pr0.3Ba0.3MnO3 compound,» *Journal of Applied Physics,* vol. 127, p. 093902, March 2020.

[45] N. Yigiter, M. Pektas, V. S. Kolat, T. Izgi, N. Bayri, H. Gencer y S. Atalay, «Structural, magnetic, and magnetocaloric properties of (1-x)La0.7Ca0.3MnO3/(x)La0.7Ag0.3MnO3 composites,» *Journal of Materials Science: Materials in Electronics,* January 2022.

[46] S. Choura-Maatar, M. M. Nofal, R. M'nassri, W. Cheikhrouhou-Koubaa, N. Chniba-Boudjada and A. Cheikhrouhou, «Enhancement of the magnetic and magnetocaloric properties by Na substitution for Ca of La0.8Ca0.2MnO3 manganite prepared via the Pechini-type sol–gel process,» *Journal of Materials Science: Materials in Electronics,* vol. 31, p. 1634–1645, December 2019.

[47] A. Sakka, R. M'nassri, M. M. Nofal, S. Mahjoub, W. Cheikhrouhou-Koubaa, N. Chniba-Boudjada, M. Oumezzine and A. Cheikhrouhou, «Structure, magnetic and field dependence of magnetocaloric properties of Pr0.5 RE0.1Sr0.4MnO3 (RE = Eu and Er),» *Journal of Magnetism and Magnetic Materials,* vol. 514, p. 167158, November 2020.

[48] K. A. Gschneidner and V. K. Pecharsky, «Magnetocaloric Materials,» *Annual Review of Materials Science,* vol. 30, p. 387–429, 8 2000.

[49] S. C. Paticopoulos, R. Caballero-Flores, V. Franco, J. S. Blázquez, A. Conde, K. E. Knipling and M. A. Willard, «Enhancement of the magnetocaloric effect in composites: Experimental validation,» *Solid State Communications,* vol. 152, p. 1590–1594, 8 2012.

[50] W. Imamura, A. A. Coelho, V. L. Kupfer, A. M. G. Carvalho, J. G. Zago, A. W. Rinaldi, S. L. Favaro and C. S. Alves, «A new type of magnetocaloric composite based on conductive polymer and magnetocaloric compound,» *Journal of Magnetism and Magnetic Materials,* vol. 425, p. 65–71, 3 2017.

S. Passanante : Investigation, Writing Original Draft,

L. P. Granja: Methodology, Supervision, Writing-Review&editing

C. Albornoz: Resources

D. Vega: Resources

D. Goijman: Resources

M. C. Fuertes: Resources

C. Ferreyra: Resources

L. Ghivelder: Formal Analysis, Resources, writing-review & editing

F. Parisi: Formal Analysis, Validation, Writing review &editing

M. Quintero: Supervision, Project administration, writing review&editing

Declaration of interests

☒ The authors declare that they have no known competing financial interests or personal relationships that could have appeared to influence the work reported in this paper.

☐ The authors declare the following financial interests/personal relationships which may be considered as potential competing interests: